FACILE SYNTHESIS OF CHAIN-LIKE NIO NANOARCHITECTURE CRYSTALS AS AN ADVANCED ELECTRODE MATERIAL FOR SUPERCAPACITORS

S. Nelson Amirtharaj[1]*, and M. Mariappan[2,] and V.Beaula premavathi[3]

Abstract

We established the chain-like NiO nanoarchitecture through CTAB assisted sonochemical synthesis process, and it is used for supercapacitor electrode application. The factors such as CTAB and ultrasound irradiation were generated the chain-like NiO crystals. The crystalline nature, internal structure, and morphological properties were characterized with X-ray diffraction analysis (XRD), Fourier transform infrared spectroscopy (FTIR), scanning electron microscopy (SEM), respectively. The NiO crystals exhibit the pseudocapacitive charge storage mechanism and provide the specific capacitance of 562 at a scan rate of 5 mV s^{-1} with good rate capability. As well, the chain-like NiO crystal retains 96 % of the initial capacitance after 3,000 cycles at a scan rate of 100 mV s^{-1}, displaying outstanding cycle stability. The easily synthesized, chain-like nanostructured, and high-performance NiO material render significant interest to sustenance for advanced energy storage devices.

Keywords: Sonochemical; CTAB; Chain-like NiO; Supercapacitors; Energy storage

[1,*3]Department of Chemistry, T. B. M. L. College (Affiliated to Bharathidasan University,Thiruchirappalli-24), Porayar, Tamilnadu 609307, India

[2]Department of Chemistry, Thiru. Vi. Ka. Govt. Arts College (Affiliated to Bharathidasan University,Thiruchirappalli-24), Thiruvarur, Tamilnadu 610003, India

***Corresponding author:** - S. Nelson Amirtharaj

*Department of Chemistry, T. B. M. L. College (Affiliated to Bharathidasan University), Porayar, Tamilnadu 609307, India Email: *snelsamir@gmail.com*

DOI: 10.48047/ecb/2023.12.si10.00261

1. Introduction

The rapidly rising energy demand and the burgeoning renewable-energy industry have fueled massive research efforts on advanced energy storage systems[1]. Recently, electrochemical energy storage devices such as supercapacitors, batteries, and fuels cells are garnering huge interest due to their accessibility, sustainability, and better performances. Among them, pseudo capacitors are attracting considerable interest in portable devices and electronic vehicles owing to their inherent combined qualities of the high energy density of chemical batteries and larger rate capability feature of traditional electrical double-layer capacitors. Furthermore, supercapacitors have several interesting characteristics, including a prolonged cycle life, reduced internal resistance, rapid charge, and discharge rates, and comparatively low cost [2–4]. Electric double-layer capacitors (EDLC) and pseudo capacitors are the two types of supercapacitors categorized based on charge storage mechanisms during the electrochemical process. The pseudo capacitors stores charges through surface redox reactions whereas EDLC store charges at the electrode and electrolyte interface through reversible adsorption of electrolyte ions. The electrode materials such as graphene oxide, activated carbon, carbon nanotube, and carbon aerogels deliver EDLC capacitance. Generally, metal oxides and conducting polymers deliver the pseudo capacitance behavior due to their redox nature[5–7]. Interestingly, pseudo capacitors render superior electrochemical properties such as high specific capacitance, good rate capability, and longer cyclic stability when compared with EDLC. Consequently, it is necessary to develop pseudo capacitor materials with favorable electrochemical properties using low-cost and environmentally benign synthetic approaches.

Till now, various transition metal oxides have been explored as supercapacitor electrode materials. Among them, ruthenium oxide has been widely explored as electrode material in pseudo capacitors, owing to its high specific capacitance of 1580 F g^{-1} and outstanding charge-discharge characteristics with strong electrical conductivity[8]. On the other hand, the commercialization of ruthenium oxide is hampered by its high cost and toxicity. In this framework, It is significant to prepare various materials such as ZnO[9], MnO_2[10], MoO_3[11], NiO[12], CuO[13], V_2O_5[14], and Co_3O_4[15] to be demonstrated as probable electrode materials for high-performance supercapacitor applications. Among them, nickel oxide (NiO) is a desirable electrode material for pseudo capacitors since its favorable features such as inexpensive and environmentally acceptable. In addition, it exhibits high theoretical capacitance (2583 F g^{-1}) within a potential of 0.5 V. NiO is a p-type semiconductor metal oxide with a broad bandgap that varies between 3.6 and 4.0 eV based on the nature and density of defects[16]. The NiO material is not only utilized in supercapacitors but also used in various fields like fuel cell catalysis[17], dye-sensitized solar cells[18], batteries[19], and sensors[20]. The electrochemical properties of nanostructured NiO differ dramatically depending on the morphologies. This is due to differences in the rate of ion migration during the electrochemical process as a function of structural morphologies.

There are various methods have been adopted to synthesize various morphologies of NiO material (hydrothermal[21], electrospinning[22], solid-state synthesis[23], and electrodeposition method[24]) for supercapacitor applications. Each synthetic approach has its strengths and drawbacks to prepare various NiO morphologies. Among them, the sonochemical approach becomes more advantageous for nanostructured materials development. The acoustic cavitation phenomena are creating various nanostructures during the sonochemical process. During acoustic cavitation, intense transitory circumstances are created which provide high temperature exceeding 5000 k, pressure surpassing 1000 atmospheres, and heating and cooling rates of more than 10^{10} k s^{-1} which could have a more impact on the structural features of prepared materials[25]. Till now, various morphologies such as nanorods [26], nanobelts [27], nanoflowers[28], and nano rice [29] have been synthesized using the sonochemical method.

In this endeavor, the chain-like NiO crystals were synthesized using a CTAB assisted sonochemical process followed by a subsequent calcination process. The CTAB is a surfactant that is extensively employed in the manufacture of crystals with regulated morphology. Furthermore, CTAB has been used as a template to alter the surface properties of NiO in order to create unique morphologies in the material. The basic properties such as crystalline behavior, nodding nature, and morphologies were demonstrated by various analytical techniques. The supercapacitor properties of the synthesized NiO crystals were examined using cyclic voltammetric (CV) and galvanostatic charge/discharge (GCD) analysis. The superior electrochemical properties make NiO a significant electrode material for supercapacitors. In addition, the synthesis process is simple and cost-effective.

2. Experimental section

2. 1. Materials

Nickel nitrate hexahydrate ($Ni(NO_3)_2.6H_2O$), ethanol, and cetyl trimethyl ammonium bromide (CTAB) were purchased from SRL (India). N-methyl-2- pyrrolidone (NMP), Carbon black, and polyvinylidene difluoride (PVDF) were acquired from Sigma Aldrich, India. Stainless steel foil, sodium hydroxide, and potassium hydroxide were obtained from Alfa aeser. Without additional purification, all reagents were also used as supplied. Throughout the experiment, deionized water was used.

2.2 Synthesis of NiO crystals

In a typical synthesis, 0.5 M of nickel nitrate hexahydrate was dissolved in 100 ml of DI water. After that 0.01 M of cetyltrimethylammonium bromide (CTAB) was dissolved in 100 mL of DI in a separate beaker. Then, the nickel nitrate precursor solution was slowly added into the CTAB solution and stirred for another half an hour to get the homogeneous solution. In this precursor solution, 10 ml of 2 M NaOH was added to get the precipitate and it was transferred ultrasonic bath for ultrasound irradiation. Then, the resultant products were collected using a centrifuge and washed with ethanol and water respectively. The washed samples were dried in a hot air oven at 70 °C for 12 h and it was well ground with a mortar pestle. The ground sample was calcined at 300 °C for 3h to attain the final product. The ultrasound irradiation time was varied to 0, 20 and 40 minutes to get the NiO-1, NiO-2, and NiO-3 crystals.

2.3 Material characterization and electrode preparation for supercapacitor analysis

The X-ray diffraction (XRD) data were recorded with BRUKER D8 Advance instrument with Cu-Kα radiation ((λ=0.154060 nm) operated at 45 kV, 40 mA and a scanning speed of 2º/min. The Fourier transform spectroscopic analysis (FTIR) analyses were recorded by SHIMADZU model IR Affinity 1 instrument with a wavelength range from 4000 to 400 cm^{-1}. The surface structural properties were examined using High-resolution scanning electron microscopy (F E I Quanta FEG 200 instrument). The supercapacitor properties were evaluated using the biologic instrument (model SP-150) in a three-electrode configuration comprising active materials coated stainless steel foil working electrode, saturated calomel reference electrode, and platinum foil counter electrode respectively. The 1 M KOH was used as the electrolyte for all electrochemical analyses. The active electrode was prepared by mixing active material, acetylene black, and poly (vinylidene fluoride) (80:10:10) in N-methyl-2-pyrrolidone (NMP) solvent and made a slurry. The resultant slurry was uniformly coated on the stainless-steel foil using the doctor blade method and it dried in a vacuum oven at 70 °C for 12 h. The dried electrodes were used to evaluate the supercapacitor properties. The material weight of the working electrode is approximately 3.5 mg.

3. Results and discussion

3.1 X-ray diffraction analysis

The crystalline properties and purity of prepared NiO materials such as NiO-1, NiO-2, and NiO-3 were examined by XRD and shown in figure 1. It is apparent that all the diffraction peaks are exhibit very low intensity and broad nature is confirmed that the prepared NiO materials have small size nanoparticles. The peaks located at 2θ=37.3, 43.5, 62.23, 75.21, and 79.23º can be related with (111), (200), (220), (311), and (222) crystal planes of the NiO crystals, respectively. The diffraction peaks of NiO materials confirm the formation of the face-centered cubic (FCC) crystalline structure of NiO materials and it is indexed with JCPDS card number-04-0835. All the XRD patterns show that the materials contain only FCC cubic NiO material and no impurities were found which confirmed that the high purity materials were attained through the present CTAB assisted sonochemical method.

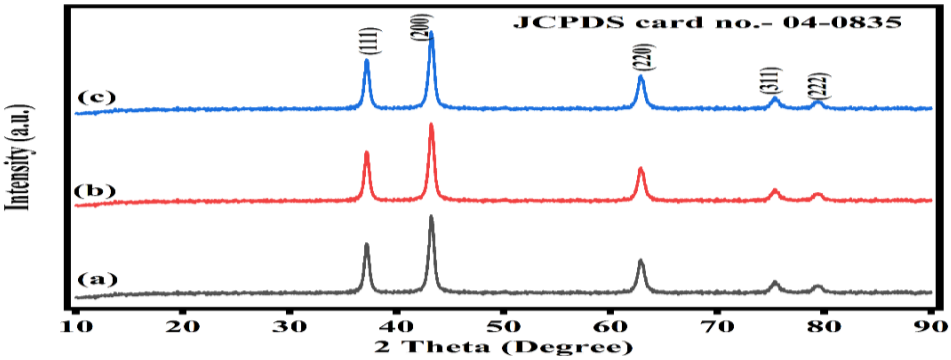

Figure 1: XRD analysis of (a) NiO-1; (b) NiO -2 and (c) NiO -3 crystals

3.2 FTIR analysis

FTIR spectral studies were done to evaluate the internal properties and bonding features of NiO crystals, as shown in the figure. 2. Three peaks at 414, 571, and 1034 cm^{-1} are the characteristic peaks of NiO materials. The peak that appeared at 414 cm^{-1} is due to the stretching vibration of Ni-O bond in NiO material, whereas 571 cm^{-1} corresponds to the bending vibration of Ni with hydroxide entities. The peak located at 1034 cm^{-1} is ascribed to the characteristic stretching vibration of SO_4 entities which came from CTAB template[30]. The XRD and FTIR studies confirm the formation of NiO crystals by CTAB assisted sonochemical synthetic approach.

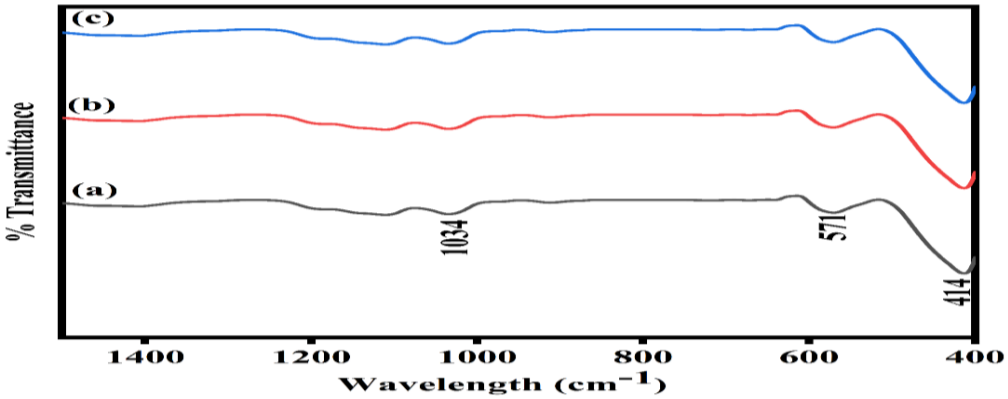

Figure 2: FTIR analysis of (a) NiO-1; (b) NiO -2 and (c) NiO-3 crystals

3.3 Morphological analysis

The morphology of the freshly prepared NiO crystals was examined by HR-SEM analysis as shown in figure 3. Figure 3 a and b show the lower and higher magnification SEM images of NiO-1 material, which was synthesized without ultrasound irradiation time. The granular shape is perfectly visible in the SEM images with an average size of 120 ±10 nm. The small nanoparticles with the size of 10 nm are also visible in SEM images. When increasing of ultrasound irradiation time to 20 min. (NiO-2) the chain-like NiO structures are formed as shown in Figures 3 c and d. The size of the chain is approximately 260 ± 10 nm. It is perfectly visible that the small granular-shaped nanoparticles are combined in a specific way and formed as chain-like structures. The cavities also formed between the chain, which is very useful for supercapacitor application. The size and particles of the chains getting increased when the ultrasound irradiation time increased to 40 minutes (NiO-3) as shown in Figures 3 e and f. In addition, the agglomeration of particles also getting increased. These results confirm that the ultrasound irradiation time and CTAB template have more influence on the morphological properties of NiO crystals.

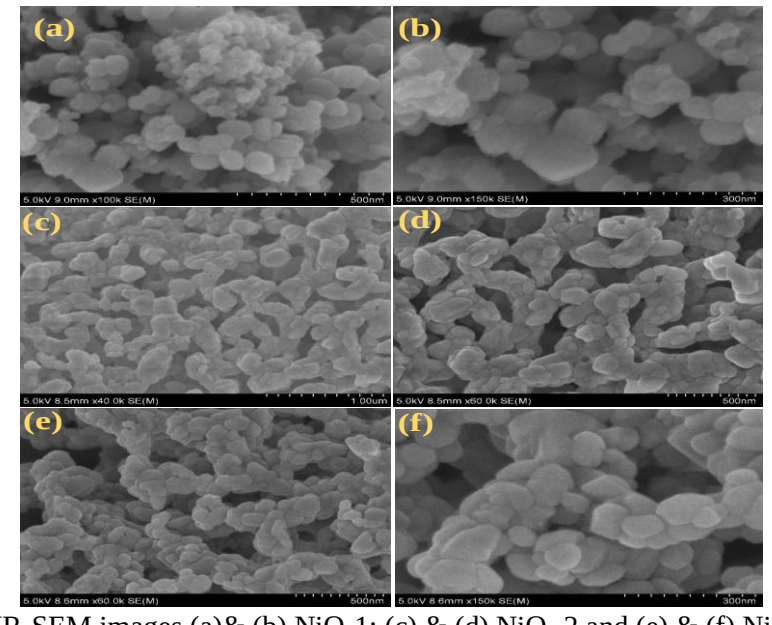

Figure 3: HR-SEM images (a)& (b) NiO-1; (c) & (d) NiO -2 and (e) & (f) NiO-3 crystals

3.4 Electrochemical analysis

To investigate the probable application of NiO in supercapacitors, the electrochemical properties of NiO materials were studied. A three-electrode electrochemical setup was used to examine the electrochemical characteristics of NiO crystals.

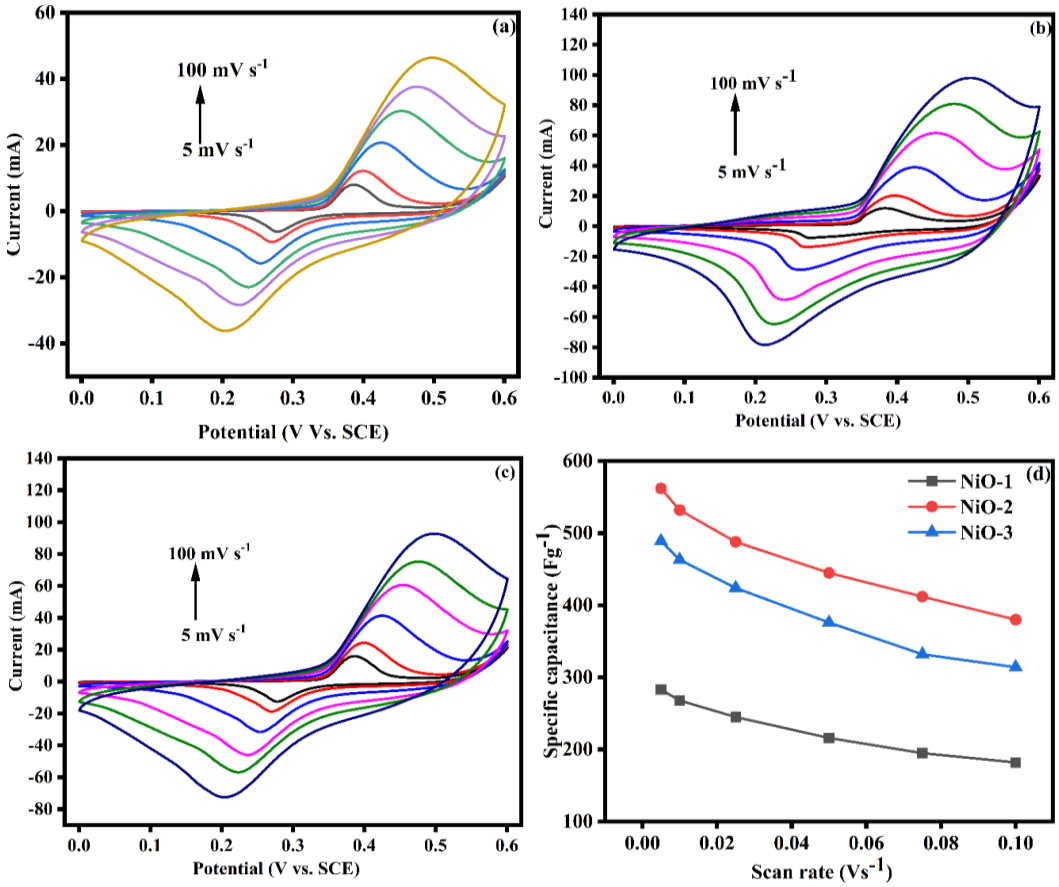

Figure 4: CV analysis of (a) NiO-1; (b) NiO -2, (c) NiO-3 crystals and specific capacitance vs scan rate graph

The electrochemical characteristics were tested using standard CV and GCD techniques in a 1 M KOH electrolyte. The CV curves of NiO crystals were shown in fig 4 (a-c). and it displays the redox peaks which suggests that the specific capacitance of the materials is mainly connected with the faradaic pseudo capacitor charge storage mechanism and the electron transfer is reversible. The anodic peak corresponds to the transformation of NiO to NiOOH in alkali electrolytes, whereas the cathodic peak is connected to the reverse reaction process. These anodic and cathodic peaks are confirming the transformation of oxidation states in NiO according to the following equation 1[31].

$$NiO + OH^- \leftrightarrow NiOOH + e^- \quad (1)$$

The shape profiles of the CV curves do not alter significantly when the scan rate raises from 5 to 100mV s^{-1}, which indicates that the electrode material has an excellent electrochemical reactivity and quick activation, implying that it has a superior electrical conductivity. The value of redox potentials moves in more positive and negative positions as the sweep rate increase. This is due to the stronger electric polarization and irreversible processes that occur at a faster scan rate[32]. Electronic neutralization will not be satisfied even during the electrochemical reaction process, since this redox reaction is restricted by the rate of ion diffusion during the electrochemical analysis[33]. The area under the CV curves is directly proportional to the specific capacitance electrode materials. Among all the NiO electrodes, NiO-2 shows the high area under the CV curve confirming the excellent supercapacitor behavior. The specific capacitance of the curves is calculated using equation (2).

$$Cs = \frac{\int idv}{2*S*M*V} \quad (2)$$

Where *Cs* is the specific capacitance in Fg^{-1}, M is the active mass (g), $\int idV$ is the integrated area, S is

the scan rate (mV s^{-1}), and V is the voltage window (V). The NiO-1, NiO-2, and NiO-3 electrodes delivered the specific capacitance of 283, 489, and 562 F g^{-1} respectively at a scan rate of 5mV s^{-1}. It is interesting to note that the NiO-2 materials deliver higher specific capacitance than the NiO-1 and NiO-3 electrodes. The superior specific capacitance performance may be ascribed to the following factors: (i) In the Chain-like nanostructures, the particles have close contact with the neighborhood particles and it provides a continuous electron transport route, which is favorable for improved electrochemical performance. (ii) The NiO crystals facilitate the rapid electron transfer during the electrochemical process due to their high conductivity. (iii) The smaller NiO nanoparticles provide the more reactive centers for faradaic redox reaction, which enhances the specific capacitance properties of the electrode materials. The NiO-3 nanoparticles deliver a lower capacitance than NiO-2, which is due to a more aggregated structure. This type of structure does not allow the electrolyte ions into the inner side of materials and reduces the specific capacitance. The rate capability of the NiO materials was analyzed through the plotting of scan rate vs specific capacitance graph as shown in fig 4 d. It demonstrated that when the scan rate increases, the specific capacitance drops. The ion exchange process can explain the decrease in specific capacitance. When the scan rate is low, the OH^- ions have adequate time to diffuse into the NiO materials, however, when the scan rate is high, the ions have much less time to approach the electrode material[34].

GCD studies were conducted in 1 M KOH solution using a Pt foil as the counter electrode and saturated calomel electrode as the reference electrode to further analyze the electrochemical characteristics and applicability of the chain-like NiO nanoparticles such as NiO-1, NiO-2, and NiO-3 are shown in figure 5 (a-c). All the charge-discharge curves display the non-linear behavior and it varies with the profile of the EDLC mechanism, confirming the pseudo capacitance charge storage behavior. This trend is comparable with the CV analysis. The lower iR drop confirms the superior pseudocapacitive behavior of the NiO materials. Among all the electrodes, NiO-2 delivers high discharge time than NiO-1 and NiO-3 crystals, confirming the excellent supercapacitor behavior of the NiO-2 materials. The specific capacitance is calculated from GCD curves using Equation (3).

$$Cs = \frac{I\Delta t}{m\Delta V} \qquad (3)$$

Where I is the input current density (Ag^{-1}), Δt is the discharge time (s) in the GCD curves, m is the weight of active electrode material and ΔV is the potential window. The NiO electrodes such as NiO-1, NiO-2, and NiO-3 are providing the specific capacitance of 282, 448, and 520 Fg^{-1}respectively at a current density of 1 A g^{-1}. The specific capacitance vs current density graph of all NiO electrodes is shown in fig 5 d.

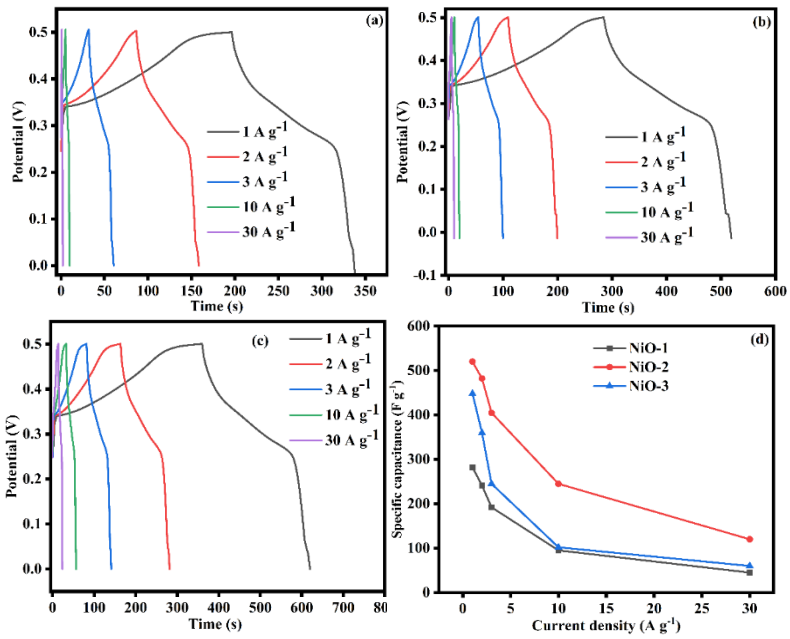

Figure 5: GCD analysis of (a) NiO-1; (b) NiO -2, (c) NiO-3 crystals and specific capacitance vs current density graph

The specific capacitance values are gradually getting lower when raising the current density from 1 to 30 Ag^{-1}. This is in good accordance with the CV curves' results. The decrease in specific capacitance as the discharge current increases is comparable to the capacitance fluctuation trend observed in CV experiments. The energy and power density parameters of the electrode materials are significant for supercapacitor application. Energy and power densities are significant factors for supercapacitor application. The energy and power densities were calculated using equations (4) and (5). and the resultant Regone plot is shown in Fig. 6.

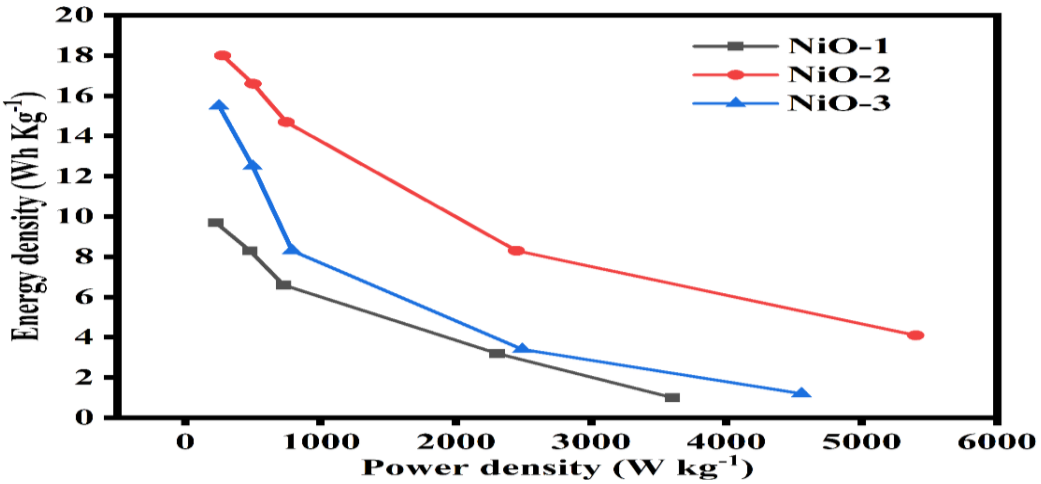

Figure 6: Ragone plot of NiO crystals

$$E = \frac{1}{2}\frac{C \times V^2}{3.6} \qquad (5)$$

$$P = \frac{E \times 3600}{t} \qquad (6)$$

Where E is energy density (Wh Kg^{-1}), C is the specific capacitance from GCD curves (F g^{-1}), V potential window (V), P power density (W Kg^{-1}), and t is the discharge time (in seconds). The NiO-1, NiO-2, and NiO-3 electrodes deliver the energy density of 9.7, 18, and 15.5 Wh Kg^{-1}. respectively at a current density of 1 Ag^{-1} whereas it exhibits the power densities of 3600, 5400, and 4555 W Kg^{-1}respectively. Cycling efficiency is another important consideration in demonstrating the supercapacitors for a variety of applications. In this endeavor, the long-time cyclic stability of the NiO electrodes was examined by repeating the CV analysis at a scan rate of 100 mVs^{-1} for 3000 cycles as shown in fig 7 a.

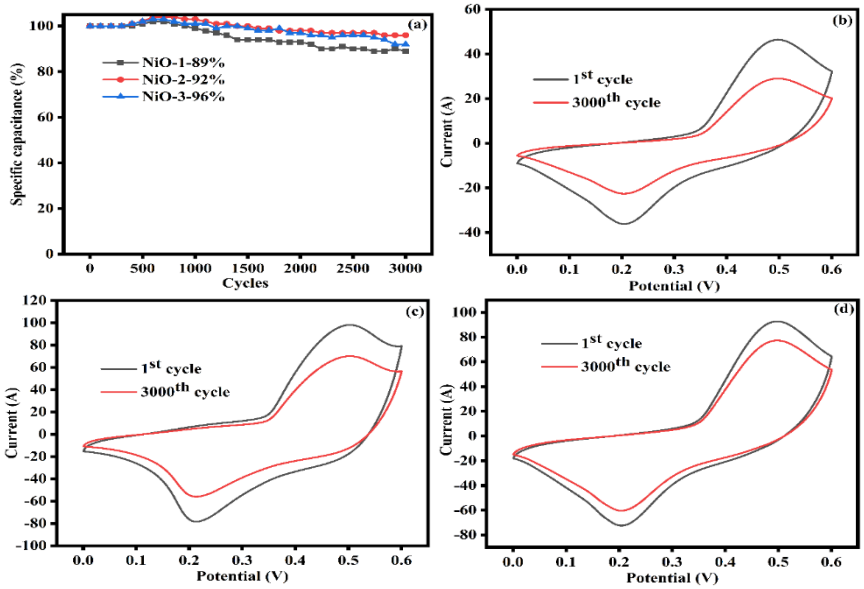

Figure 7: (a) Cycle life test of NiO crystals at a scan rate of 100 mV s^{-1}. 1st and 3000th CV curves of (a) NiO-1; (b) NiO-2 and (c) NiO -3 materials

In addition, figure 7 b, c, and d show the 1st and 3000th cycles of cyclic stability analyses of NiO-1, NiO-2, and NiO-3 electrodes respectively. It is obvious that the specific capacitance retention of NiO electrodes steadily increases at initial cycles, then declines slowly. This signifies that the electrode is being activated during initial cycles of cyclic stability analysis[35]. The overall initial capacitance loss for NiO-1, NiO-2, and NiO-3 electrodes are11, 4, and 8 % respectively. Among all the electrodes, NiO-2 demonstrates superior cyclic stability performance with 96 % of initial specific capacitance retention. The chain-like NiO material (NiO-2) exhibits outstanding supercapacitor characteristics with excellent specific capacitance and good long-term cyclic stability when examined as a supercapacitor electrode material.

4. Conclusion

In summary, a simple, cost-effective synthetic method has been adopted for the preparation of NiO nanostructures for supercapacitor electrode application. The ultrasound irradiation and CTAB template are the two significant parameters to generate the chain-like NiO nanoarchitecture. The chain-like NiO nanostructure not only renders a high surface area but also gives a pathway for continuous electron transport route for electrolyte ion during the electrochemical process. As prophesied, the resulting chain-like NiO structure (NiO-2) delivered a high specific capacitance of 562 F g^{-1} at a scan rate of 5 mV s^{-1} with excellent rate capability and cyclic stability, which reveal the applicability for supercapacitor device application.

References

1. Peng H, Ma G, Mu J et al 2014 Low-cost and high energy density asymmetric supercapacitors based on polyaniline nanotubes and MoO_3 nanobelts *J Mater Chem A* **2** 10384
2. Amaresh S, Karthikeyan K, Jang I C, Lee Y S 2014 Single-step microwave mediated synthesis of the CoS_2 anode material for high rate hybrid supercapacitors *J Mater Chem A* **2** 11099
3. Chen W, Rakhi R B, Hedhili M N, Alshareef H N 2014 Shape-controlled porous nanocarbons for high performance supercapacitors *J Mater Chem A* **2** 5236
4. Wang R, Yan X, Lang J, et al 2014 A hybrid supercapacitor based on flower-like $Co(OH)_2$ and urchin-like VN electrode materials *J Mater Chem A* **2** 12724
5. Pettong T, Iamprasertkun P, Krittayavathananon A, et al 2016 High-Performance Asymmetric Supercapacitors of $MnCo_2O_4$ Nanofibers and N-Doped Reduced Graphene Oxide Aerogel *ACS Appl Mater Interfaces* **8** 34045
6. Radhamani A V., Shareef K M, Rao M S R 2016 ZnO@MnO_2 Core-Shell Nanofiber Cathodes for High Performance Asymmetric Supercapacitors *ACS Appl Mater Interfaces* **8** 30531
7. Chen J S, Guan C, Gui Y, Blackwood D J 2017 Rational design of self-supported Ni_3S_2 nanosheets array for advanced asymmetric supercapacitor with a superior energy density *ACS Appl Mater Interfaces* **9** 496
8. Hu C C, Chang K H, Lin M C, Wu Y T 2006 Design and tailoring of the nanotubular arrayed architecture of hydrous RuO_2 for next generation supercapacitors *Nano Lett* **6** 2690
9. Luo Q, Xu P, Qiu Y, et al 2017 Synthesis of ZnO tetrapods for high-performance supercapacitor applications *Mater Lett* **198** 192
10. Zhao S, Liu T, Hou D, et al 2015 Controlled synthesis of hierarchical birnessite-type MnO_2 nanoflowers for supercapacitor applications *Appl Surf Sci* **356** 259
11. Li J, Liu X 2013 Preparation and characterization of α-MoO_3 nanobelt and its application in supercapacitor *Mater Lett* **112** 39
12. Dar F I, Moonooswamy K R, Es-Souni M 2013 Morphology and property control of NiO nanostructures for supercapacitor applications *Nanoscale Res Lett* **8** 1
13. Shinde S K, Yadav H M, Ghodake G S, et al 2019 Using chemical bath deposition to create nanosheet-like CuO electrodes for supercapacitor applications *Colloids Surfaces B Biointerfaces* **181**1004
14. Yang J, Lan T, Liu J, et al 2013 Supercapacitor electrode of hollow spherical V2O5 with a high pseudo capacitance in aqueous solution *Electrochim Acta* **105** 489
15. Xia X H, Tu J P, Mai Y J, et al 2011 Self-supported hydrothermal synthesized hollow Co_3O_4 nanowire arrays with high supercapacitor capacitance *J Mater Chem* **21** 9319
16. Wang H, Yi H, Chen X, Wang X 2013 Facile synthesis of a nano-structured nickel oxide electrode with outstanding pseudocapacitive properties *Electrochim Acta* **105** 353
17. Czelej K, Cwieka K, Colmenares J C, Kurzydlowski K J 2018 Catalytic activity of NiO cathode in molten carbonate fuel cells

Appl Catal B Environ **222** 73
18. Li N, Gibson EA, Qin P, et al 2010 Dou ble-layered NiO photocathodes for p-Type DSSCs with record IPCE *Adv Mater* **22** 1759
19. Wang X, Yang Z, Sun X, et al 2011 NiO nanocone array electrode with high capacity and rate capability for Li-ion batteries *J Mater Chem* **21** 9988
20. Huran J, Spiess L 2000 Preparation and characterization of NiO thin films for gas. **58** 300
21. Justin P, Meher S K, Rao G R 2010 Tuning of capacitance behavior of NiO using anionic, cationic, and nonionic surfactants by hydrothermal synthesis *J Phys Chem C* **114** 5203
22. Liu S, Jia J, Wang J, et al 2012 Synthesis of Fe-doped NiO nanofibers using electrospinning method and their ferromagnetic properties *J Magn Magn Mater* **324** 2070
23. Salavati-Niasari M, Mohandes F, Davar F, et al 2009 Preparation of NiO nanoparticles from metal-organic frameworks via a solid-state decomposition route. *Inorganica Chim Acta* **362** 3691
24. Wu M S, Huang Y A, Yang C H, Jow J J 2007 Electrodeposition of nanoporous nickel oxide film for electrochemical capacitors *Int J Hydrogen Energy* **32** 4153
25. Hangxun X, Zeiger B W, Suslick K S 2013 Sonochemical synthesis of nanomaterials *Chem Soc Rev* **42** 2555
26. Kianpour G, Salavati-Niasari M, Emadi H 2013 Sonochemical synthesis and characterization of $NiMoO_4$ nanorods. *Ultrason Sonochem* **20** 418
27. Chen YJ, Meng FN, Yu HL, et al 2013 Sonochemical synthesis and ppb H_2S sensing performances of CuO nanobelts *Sensors Actuators, B Chem* **176**:15
28. Qi C, Zhu Y J, Wu C T, et al 2016 Sonochemical synthesis of hydroxyapatite nanoflowers using creatine phosphate disodium salt as an organic phosphorus source and their application in protein adsorption *RSC Adv* **6** 9686
29. Zhang M, Zhao A, Li D, et al 2012 A simple and highly efficient route to the synthesis of $NaLnF_4$-Ag hybrid nanorice with excellent SERS performances. *Analyst* **137** 4584
30. Mohamed Mohaideen H, Sheik Fareed S, Natarajan B 2019 Role of calcination temperatures on the structural and optical properties of nio nanoparticles. *Surf Rev Lett* **26** 1950043
31. Zeng Y, Wang L, Wang Z, et al 2015 Facile synthesis of self-assembled porous NiO nanostructures and their application to supercapacitor electrodes *Mater Today Commun* **5** 70
32. Chen F, Zhou W, Yao H, et al 2013 Self-assembly of NiO nanoparticles in lignin-derived mesoporous carbons for supercapacitor applications *Green Chem* **15** 3057
33. Fan L, Tang L, Gong H, et al 2012 Carbon-nanoparticles encapsulated in hollow nickel oxides for supercapacitor application *J Mater Chem* **22** 16376
34. Yesuraj J, Suthanthiraraj SA 2019 Bio-molecule templated hydrothermal synthesis of $ZnWO_4$ nanomaterial for high-performance supercapacitor electrode application *J Mol Struct* **1181** 131
35. Yesuraj J, Austin Suthanthiraraj S, Padmaraj O 2019 Synthesis, characterization and electrochemical performance of DNA-templated Bi_2MoO_6 nanoplates for supercapacitor applications *Mater Sci Semicond Process* **90** 225